001595

ORIGIN OF MULTIPLE FABRICS DURING A SINGLE FOLDING EPISODE

*(due to their ameneity to both buckle folding and layer parallel compression)

In a sequence of interbedded lithologies of variable thickness and competence, certain thin beds with intermediate competence and properties may (*) undergo a very complex strain history (bulk translation and rotation ignored), as follows:-

(i) Layer parallel compression (or layer normal thickening).

(ii) Buckle folding, involving end member strain types:-

a) body rotation with no internal strain at inflexion points and along the neutral surface

b) layer parallel extension in the outer arcs of buckles.

c) layer parallel compression in the inner arcs

(iii) Flattening of buckles involving a heterogeneous compressive strain of the layer

(iv) Higher order folding of the layer involving different parts of the layer in the strain types a) b) + c) above if the folding is of buckling type, or, if of similar type, various degrees of simple and pure shear.

(v) Further flattening, etc

(vi) Further order folding, body rotations, etc.

Given the right metamorphic conditions, tectonic fabrics may start to form during stage (i) and may be subsequently rotated and/or overprinted during stages (ii) a) and b) and intensified during (ii) c). In addition mimetic recrystallization and growth, and rotation of initial sedimentary fabrics, if present, may also occur during stages (i) and (ii). These fabrics and tectonic fabrics rotated during (ii) a) & formed during (ii) b) may be rotated and/or overprinted during (iii) and so on, giving, in the case of a multilayer as described above, a very complex rotational strain history with which recrystallization may or may not be able to keep pace. The following diagrams illustrate the possible results if recrystallization does not keep pace with rotations:-

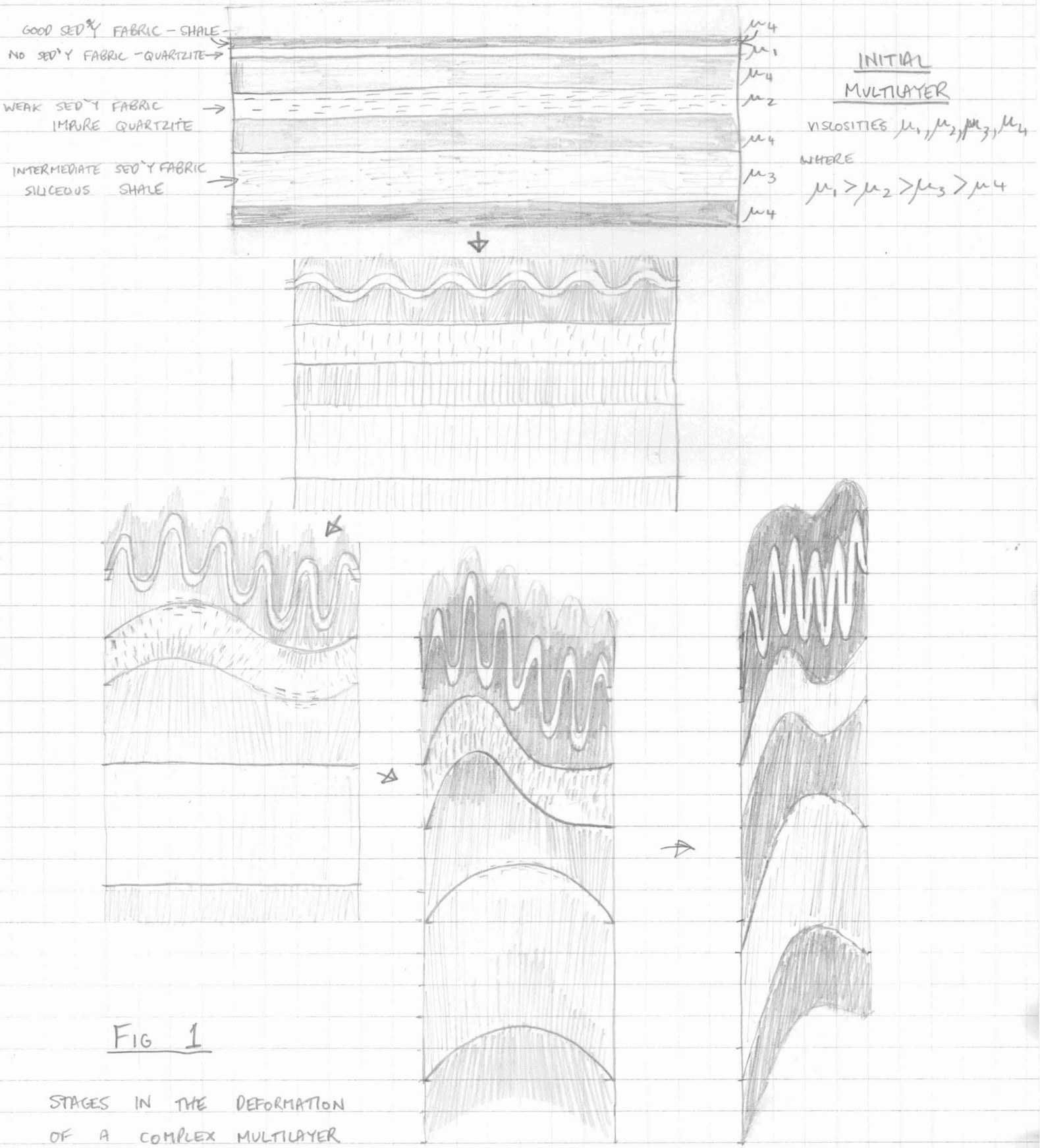

FIG 1

STAGES IN THE DEFORMATION OF A COMPLEX MULTILAYER SHOWING FABRICS THAT MAY FORM GIVEN IDEAL CONDITIONS.

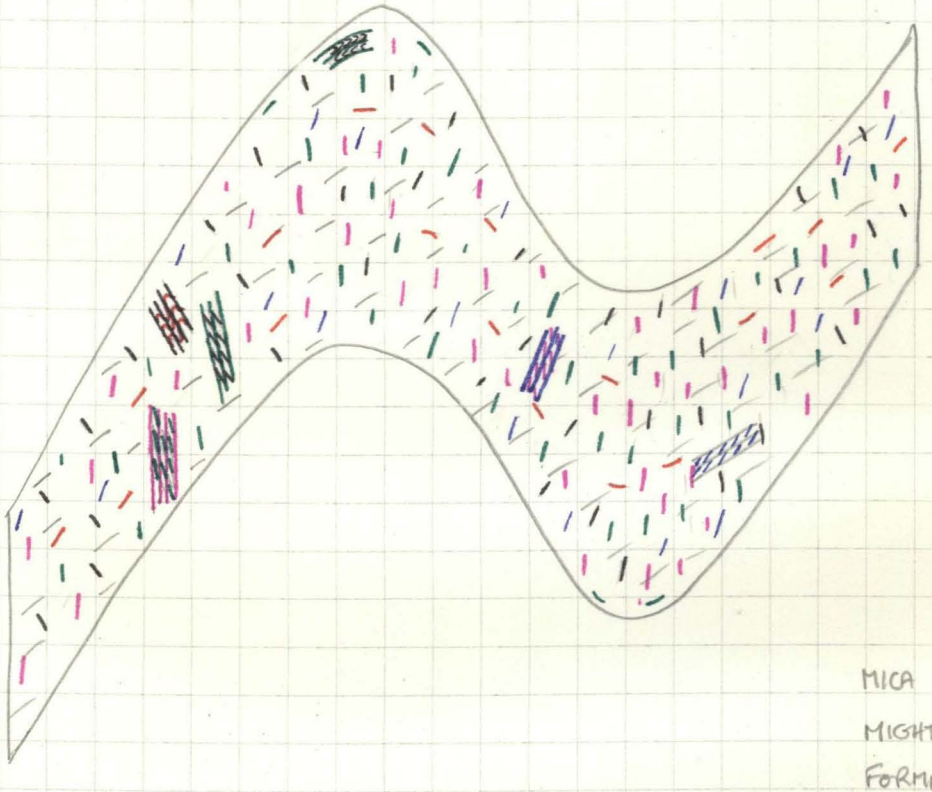

FIG 2

MICA ORIENTATIONS THAT MIGHT RESULT FROM FABRIC FORMING PROCESSES OPERATING DURING THE DEFORMATION AND METAMORPHISM OF A COMPLEX MULTILAYER

— BEDDING FABRIC
— LAYER // COMPRESSION FABRIC
— BUCKLING FABRIC
— HIGHER ORDER BUCKLING AND FLATTENING FABRIC
— SIMPLE SHEAR FABRIC
— FABRIC FORMED DURING FURTHER FLATTENING AFTER AFTER A LOCAL EXTERNAL ROTATION.

The important processes of fabric formation during deformation and metamorphism are :-

1) Preferred nucleation and growth of micas in the XY plane of the incremental strain ellipsoid*
2) Mimetic recrystallization and growth of pre-existing prefered orientations of phyllosilicates
3) Rotation of pre-existing fabrics.

For various reasons process 3 may be inhibited and in any case can never achieve complete parallelism with micas formed during process 1.

* not the finite strain ellipsoid which is an abstract quantity and may have a very different orientation.

Hence mica growth by processes 1 and 2 may give rise to and preserve a multitude of mica orientations and although fig. 2 is an unrealistically extreme example of what may result, thin layers of intermediate viscosity may exhibit some of the features shown.

Conclusion →

It must be stressed, then that the presence of local misoriented micas in a rock with an otherwise pervasive fabric need not neccessarily imply that those misoriented mica represent relics of an earlier pervasive tectonic fabric.

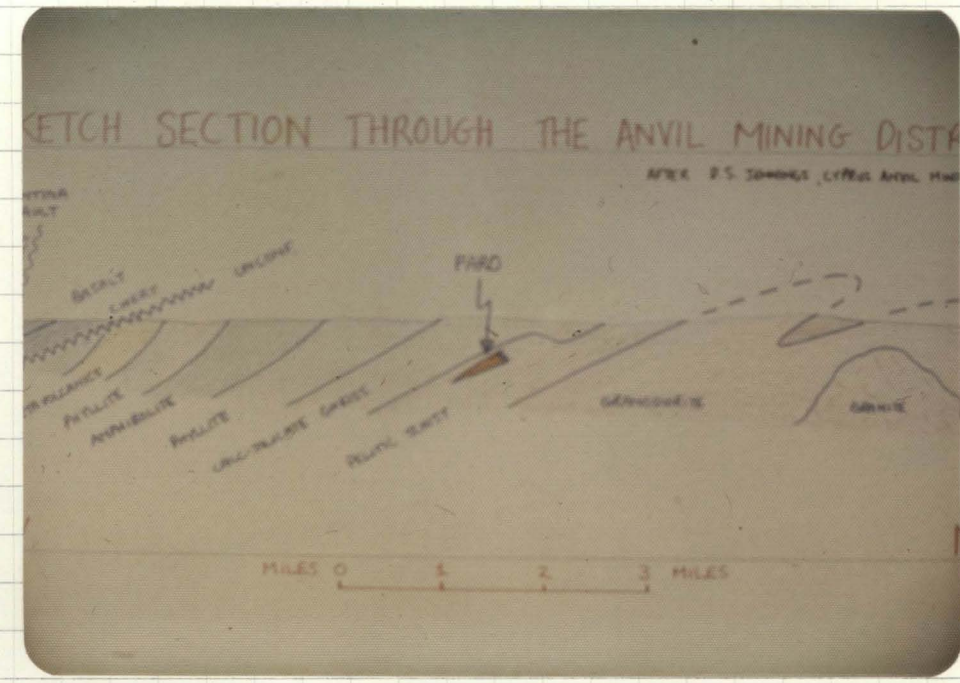
KETCH SECTION THROUGH THE ANVIL MINING DISTA
PARD
MILES 0 1 2 3 MILES

FIG 2.

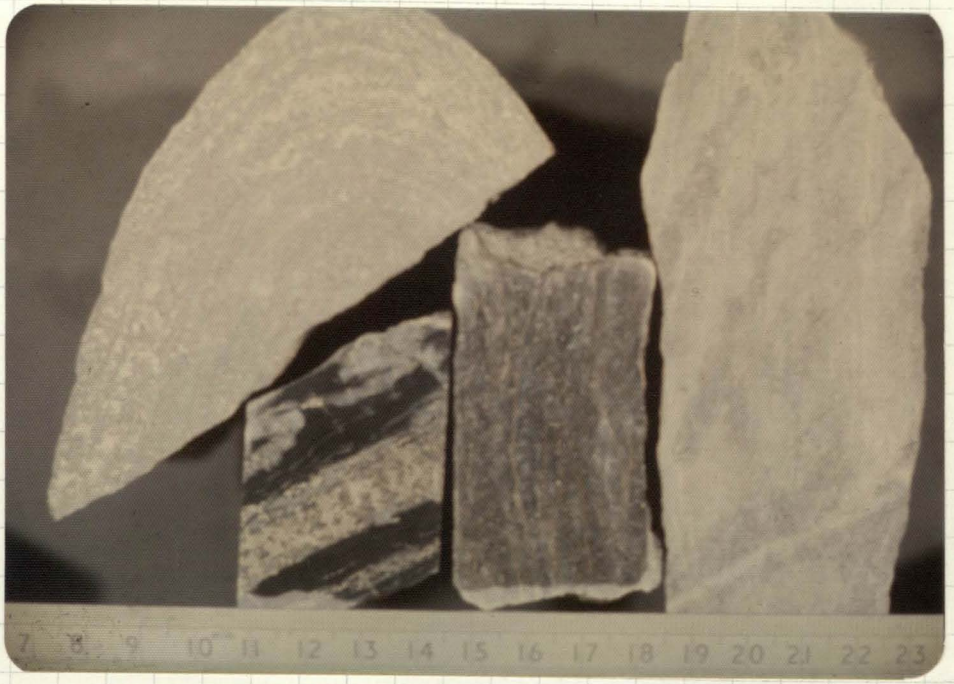

FIGURE 2

SULPHIDE-BEARING QUARTZITE.

Left to right:

a) Pyritic, with folded compositional layering, early schistosity and bedding striping (not seen).

b) Banded, graphitic, with first phase folds in the banding and transposition of banding parallel to cleavage.

c) Sphalerite-rich, in core with early schistosity sub-vertical, and parallel to compositional banding. and d) Sulphide-poor, with dark coarse-quartz bands at about 30° to the early schistosity.

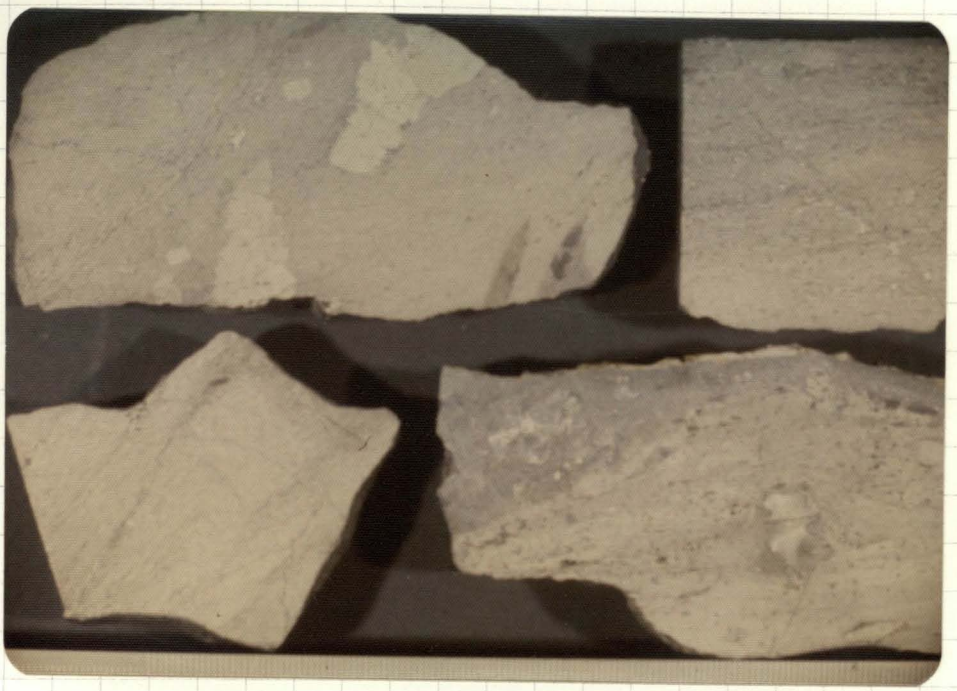

FIGURE 3

PYRRHOTITE SCHIST.

Clockwise from upper left:

a) with coarse anhedral pyrite layers, sometimes boudinaged or folded (not seen) and schistosity outlined by platy silicates,

b) with linear fabric in hand specimen (see Fig. 22) and abundant fine pyrite-marcasite,

c) with silicate fragments, and d) with 'N' symmetry fold in the schistosity

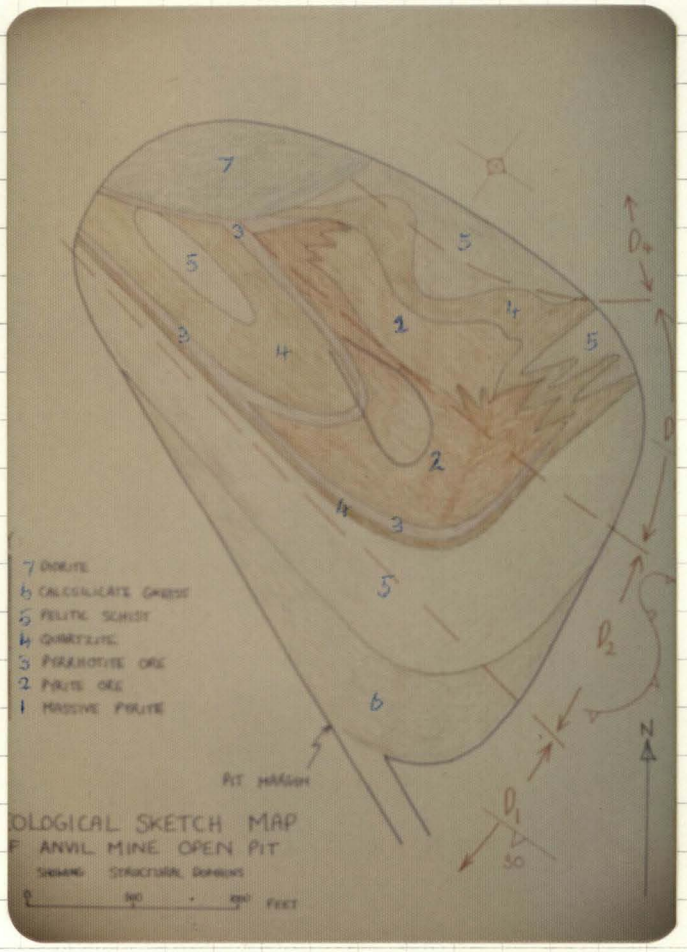
7 DIORITE
6 CALCSILICATE GNEISS
5 PELITIC SCHIST
4 QUARTZITE
3 PYRRHOTITE ORE
2 PYRITE ORE
1 MASSIVE PYRITE
PIT MARGIN
OLOGICAL SKETCH MAP
F ANVIL MINE OPEN PIT
SHOWING STRUCTURAL DOMAINS
FEET
N
30

FIGURE 4

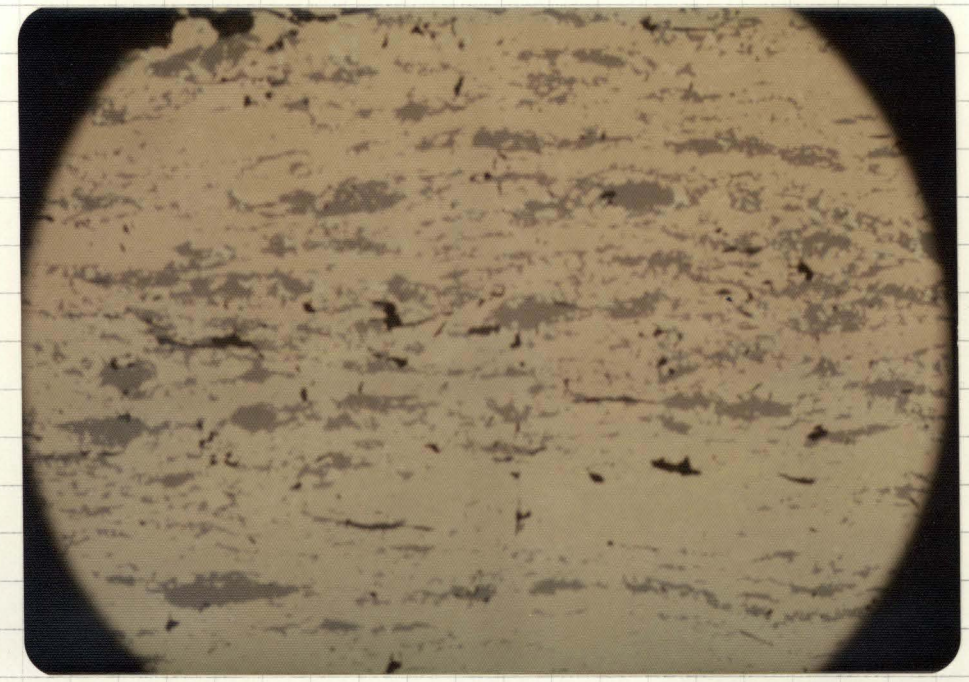

FIGURE 4

PYRRHOTITE SCHIST IN PLANE POLARIZED LIGHT, showing form orientation of sphalerite (mid grey) and silicates (dark grey)

Field of view ~ 1·5 mm.

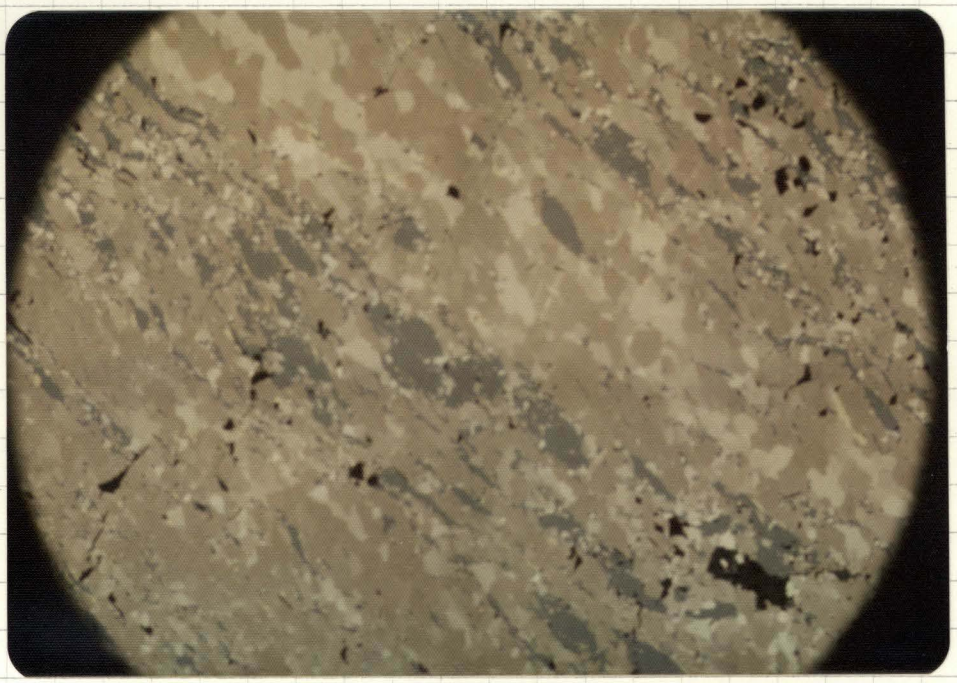

FIGURE 5

PYRRHOTITE SCHIST, VIEWED THROUGH PARTLY CROSSED NICOLS, showing most pyrrhotite in extinction (brown) and with a weak form orientation.

Field of view ~ 1·5 mm.

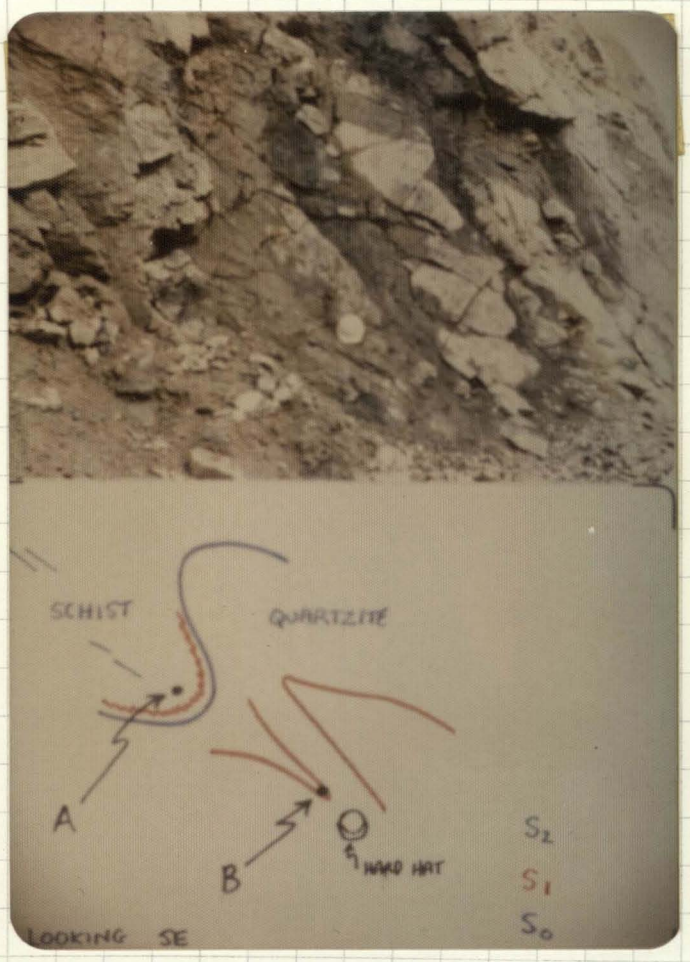

FIGURE 5

FOLDED QUARTZITE - SCHIST CONTACT IN STRUCTURAL DOMAIN 3. showing location of samples A and B

S_2 - second phase crenulation cleavage

S_1 - first phase pervasive cleavage

S_0 - lithological contact ≡ bedding

FIGURE 6

- SAMPLE B

- SAMPLE A

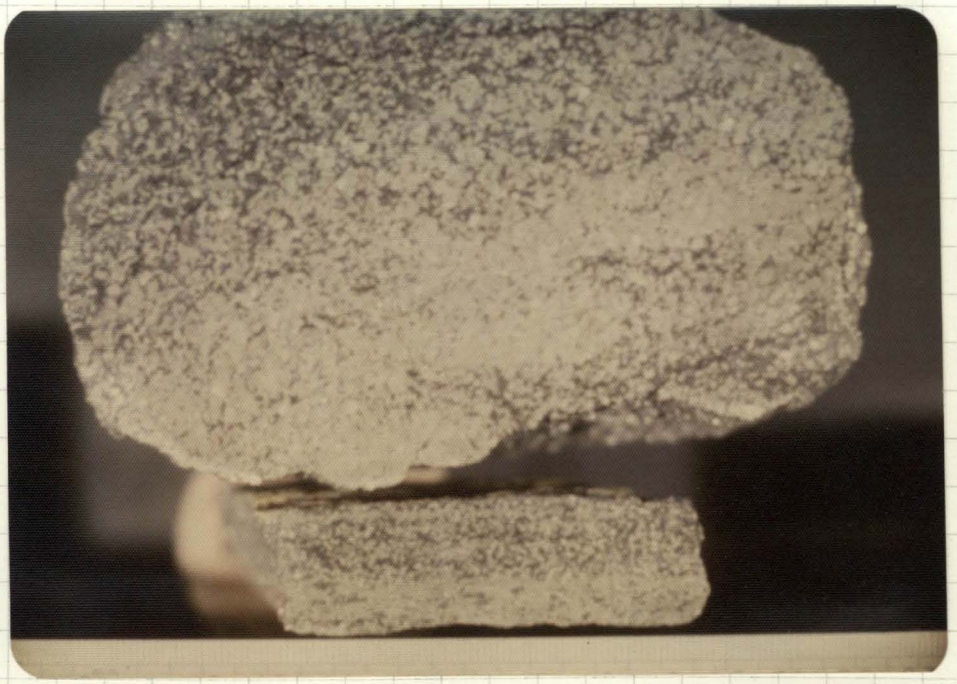

FIGURE 6
BANDED GNEISSOSE ORE, showing variable composition in bands of coarse pyrite porphyroblasts in a sphalerite-galena matrix

FIGURE 7
THE PYRITIC SULPHIDE FACIES
Clockwise from the top:
a) showing a fault polish surface with a 1 cm zone of triturated pyrite on either side
b) showing an earlier breccia texture with fragments of quartzite and banded ore
c) coarse, schistose and sandy with voids probably due to the leaching of sulphate, and d) weakly foliated and finer grained than c), with magnetite porphyroblasts.

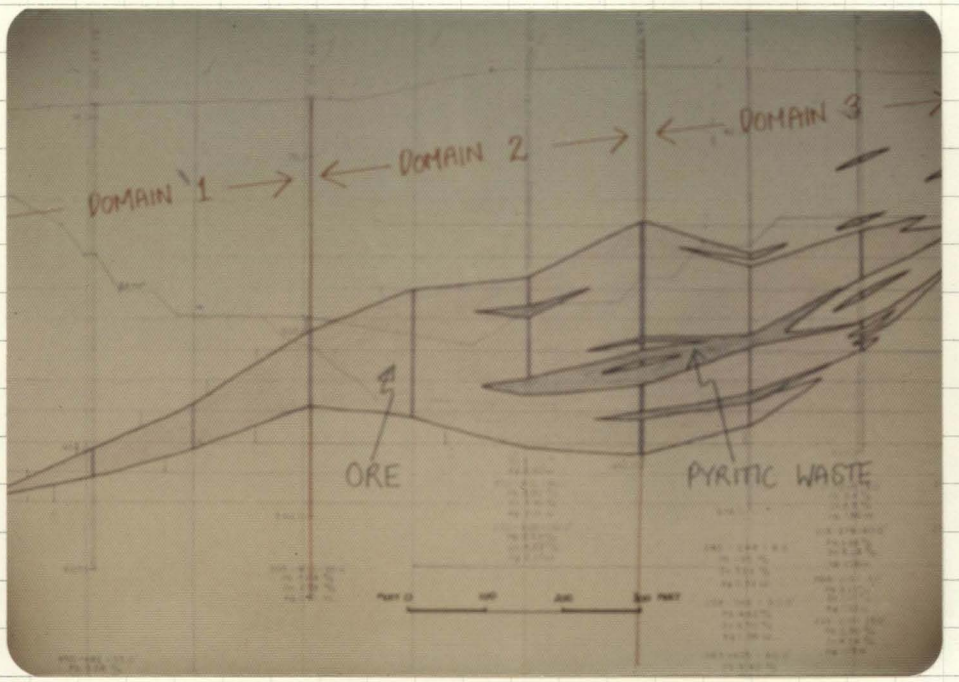

FIGURE 7 : ORE SECTION #110

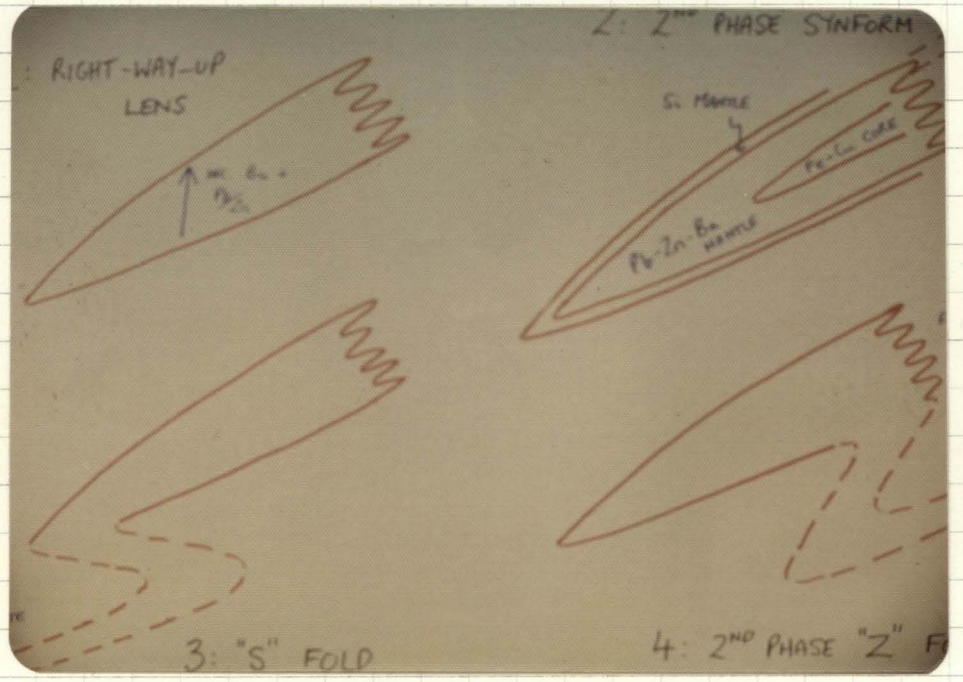

FIGURE 8 : PREVIOUS AND PRESENT HYPOTHESES

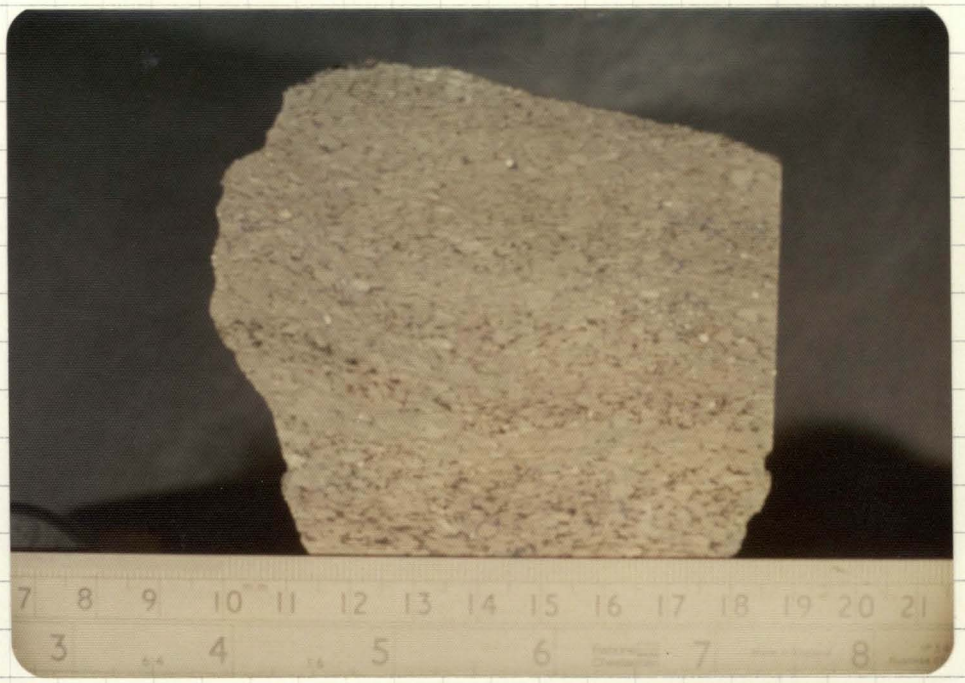

FIGURE 8
COARSE, BASE-METAL-BEARING PYRITE SCHIST, cut normal to schistosity

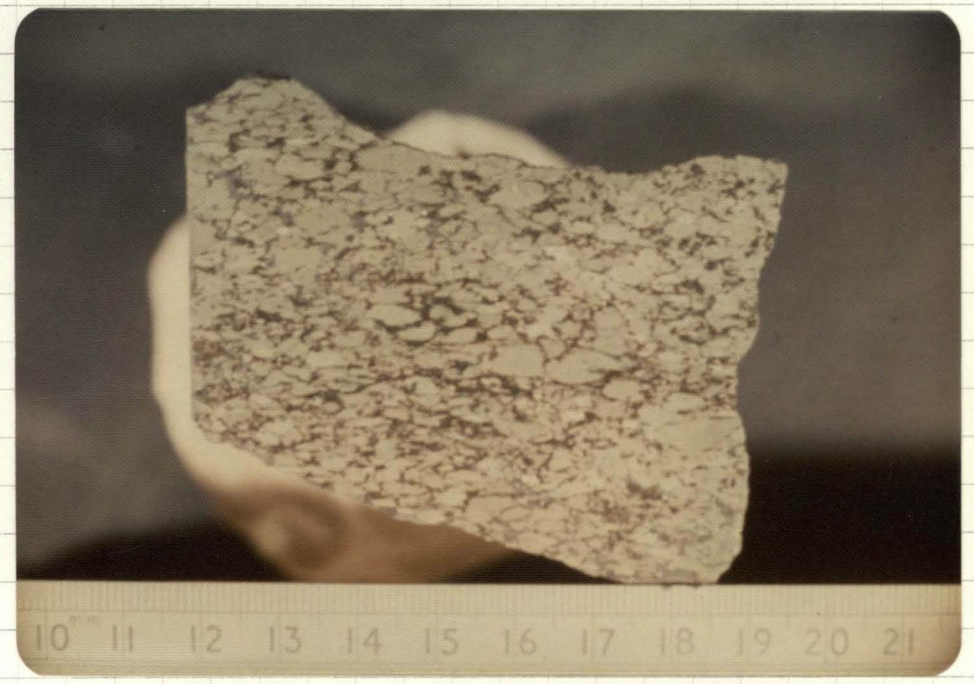

FIGURE 9
COARSE, BASE-METAL-BEARING PYRITE SCHIST, cut parallel to schistosity.

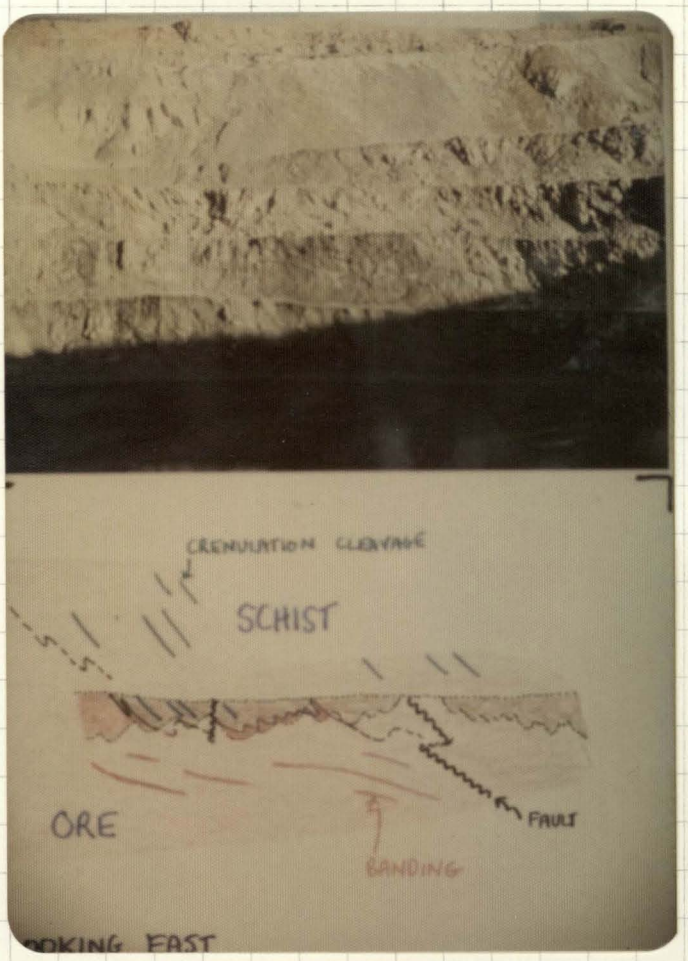

FIGURE 9

THE EAST WALL OF THE ANVIL PIT, SUMMER 1975. showing the quartzite - schist contact

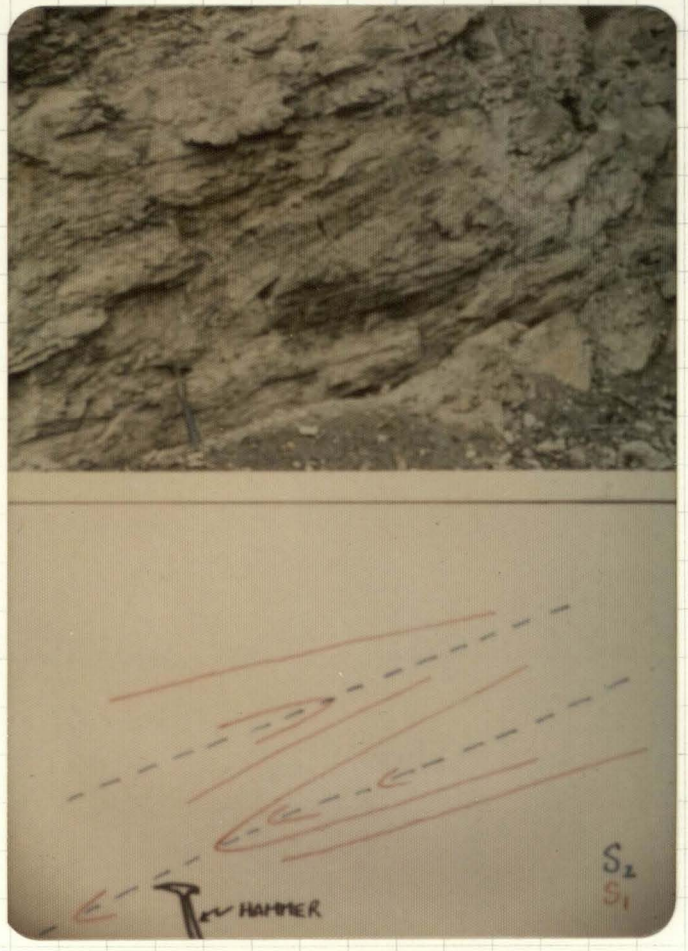

FIGURE 10

SECOND PHASE "Z" SYMMETRY FOLD IN METABASITE HORIZON, WEST WALL OF PIT

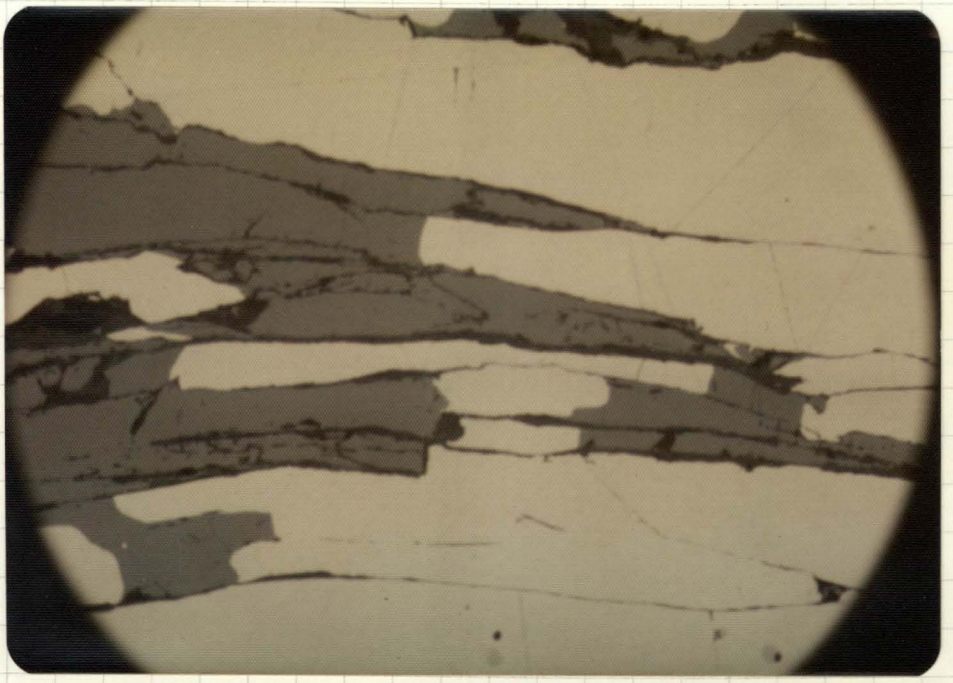

FIGURE 10
COARSE, SILICATE-BEARING PYRITE SCHIST, section normal to schistosity.

Field of view ~ 1·5 mm.

FIGURE 11
BARITIC SCHIST.
Clockwise from top left.
a) pyritolitic
b) with folded banding
c) with strong planar schistosity and banding

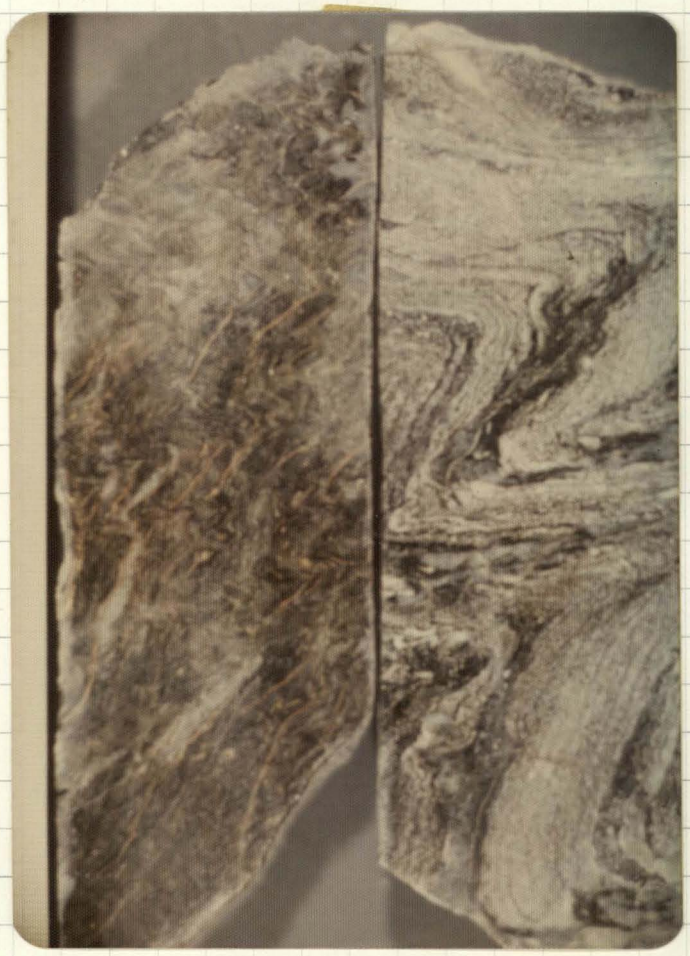

FIGURE 11

EXAMPLES OF "S" (on the left) AND "Z" SYMMETRY

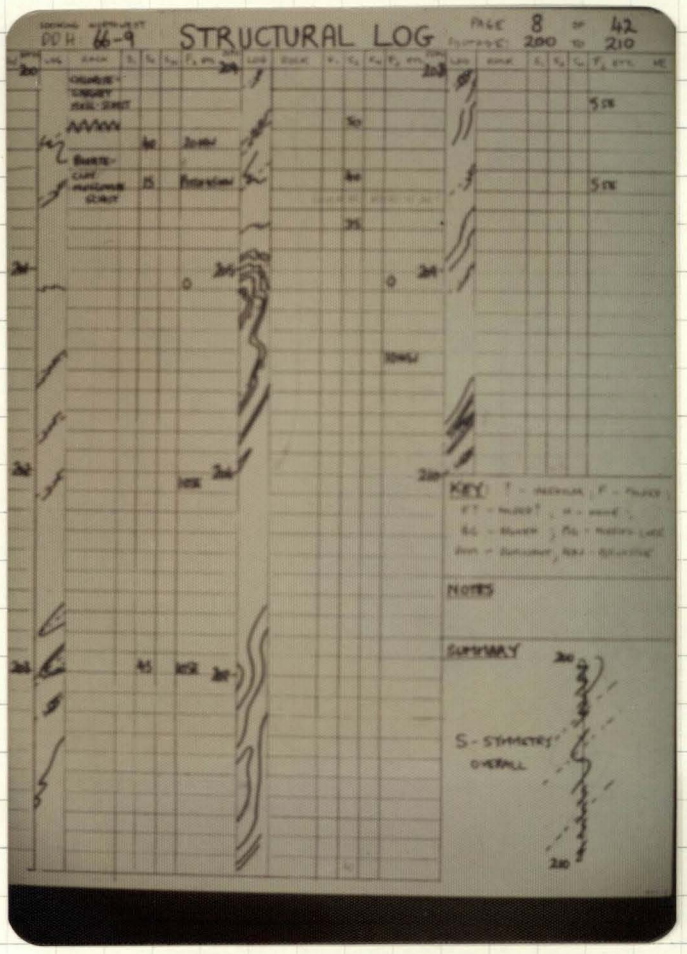

FIGURE 12

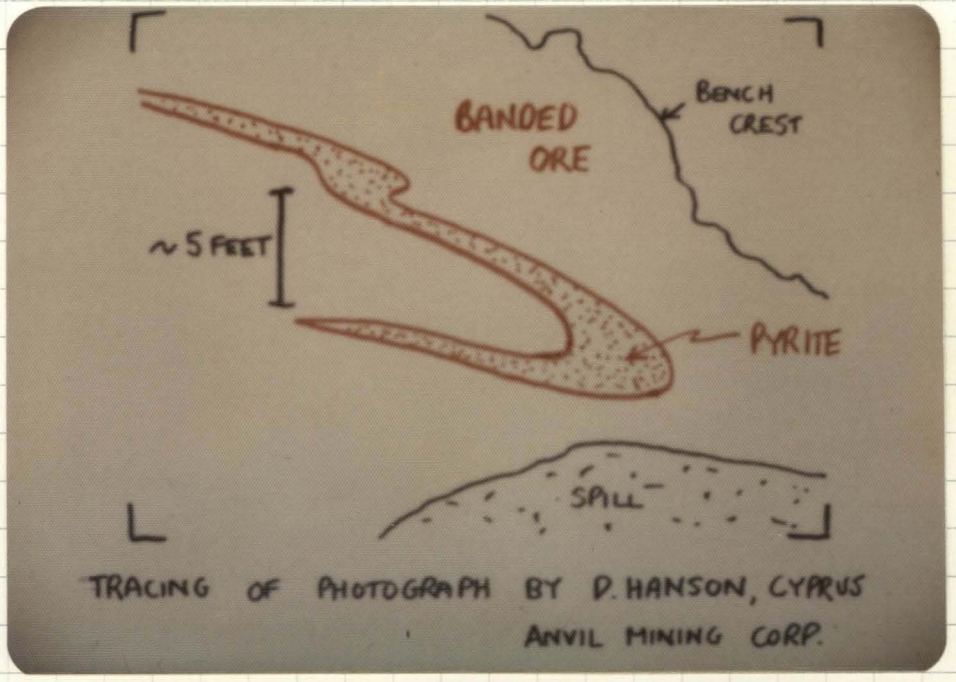

FIGURE 12
POSSIBLE FIRST PHASE FOLD IN PYRITE LAYER

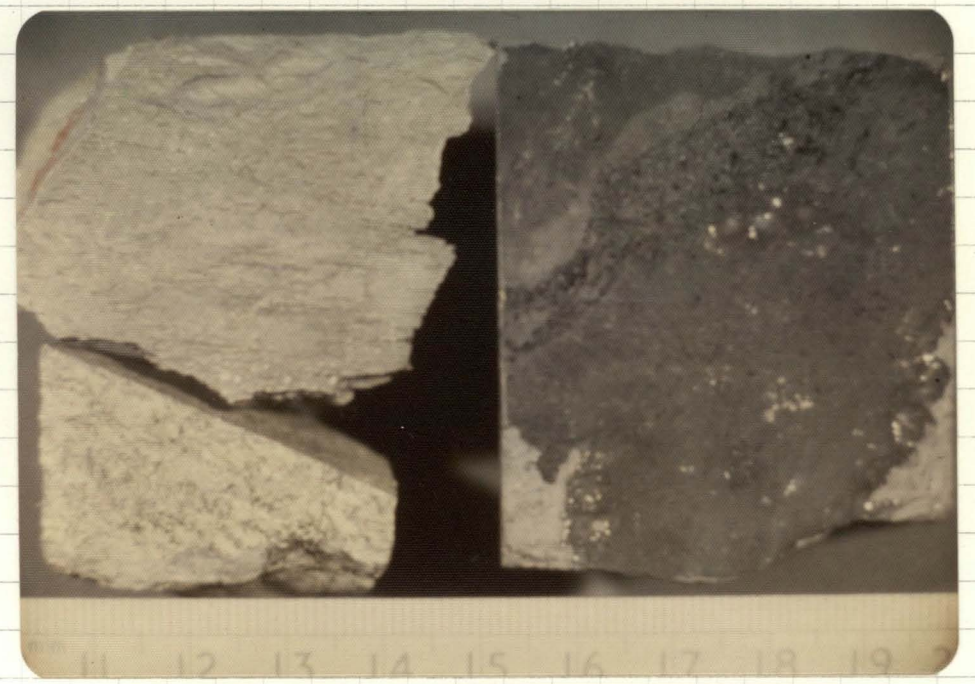

FIGURE 13
MINOR SULPHIDE/OXIDE FACIES.
Clockwise from top left:
a) fine grained pyrite-marcasite rock, now replacing pyrrhotite schist
b) magnetite-rich rock, found in association with pyrrhotite schist and,
c) chalcopyrite-pyrrhotite schist

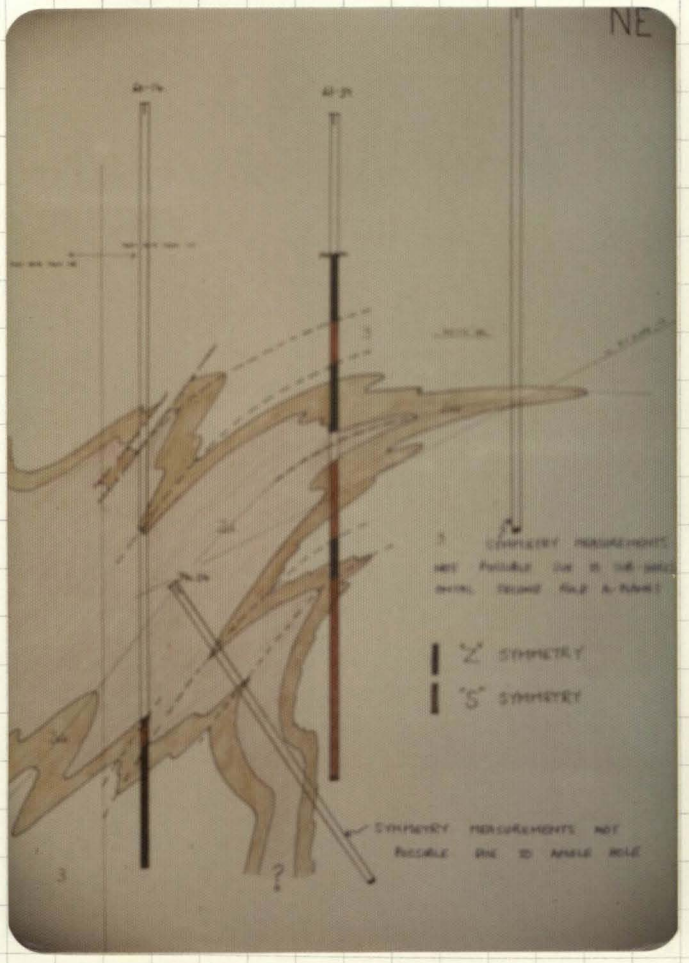

FIGURE 13

GEOLOGICAL SECTION, DOMAIN 3
SECTION 110.

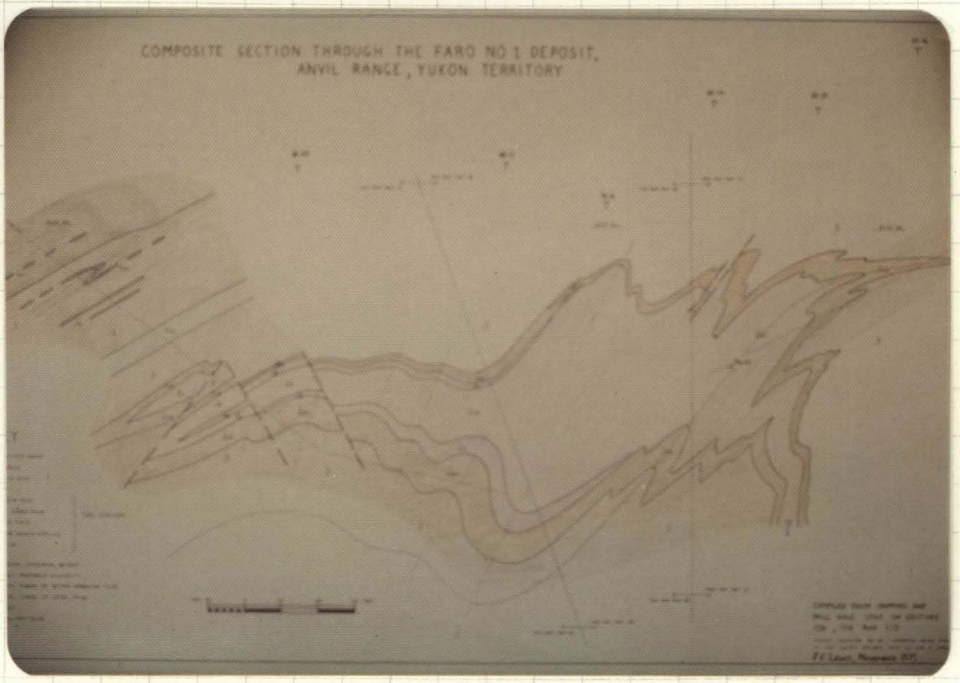

FIGURE 14

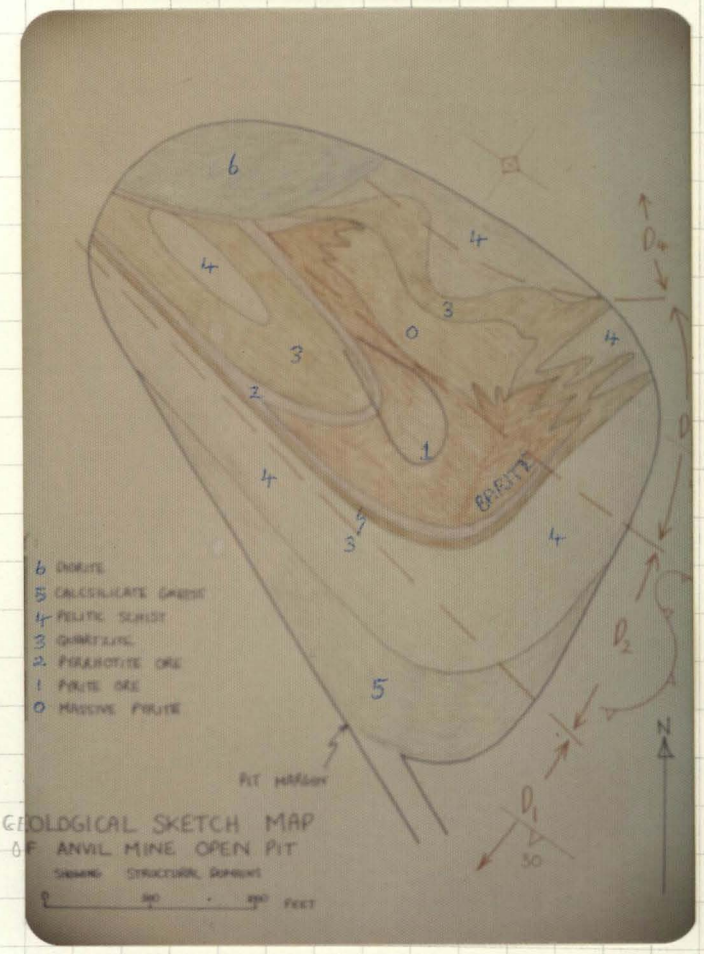

FIGURE 14

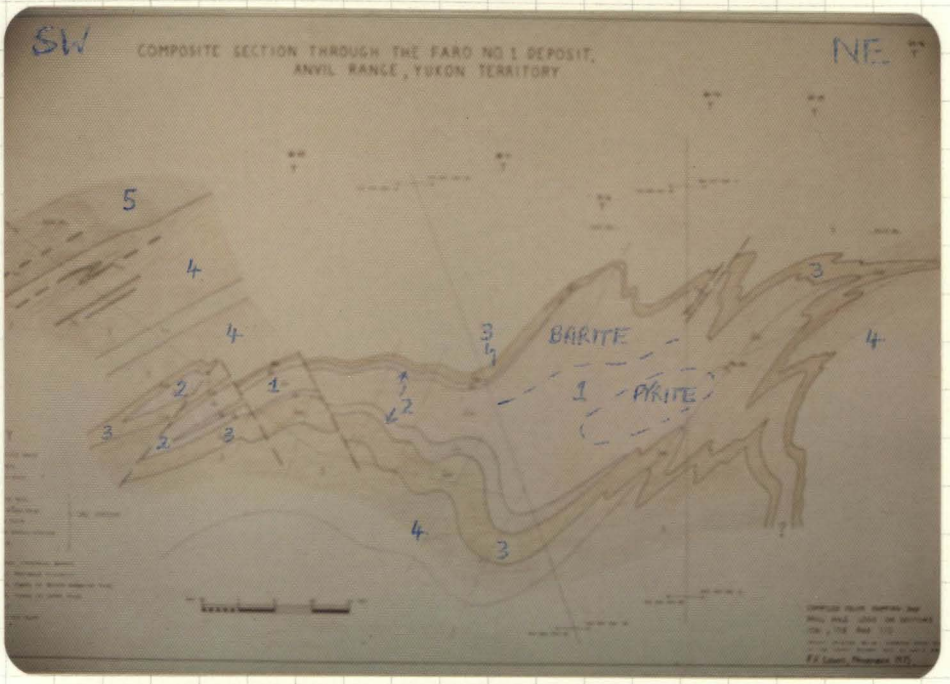

FIGURE 15

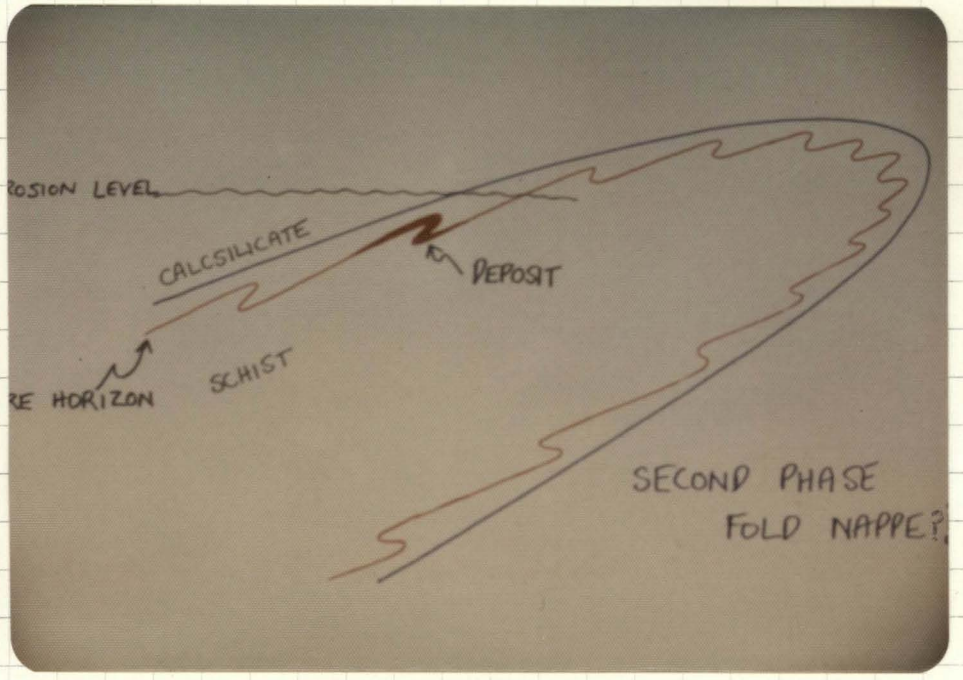
OSION LEVEL
CALCSILICATE
DEPOSIT
E HORIZON
SCHIST
SECOND PHASE
FOLD NAPPE?

FIGURE 15

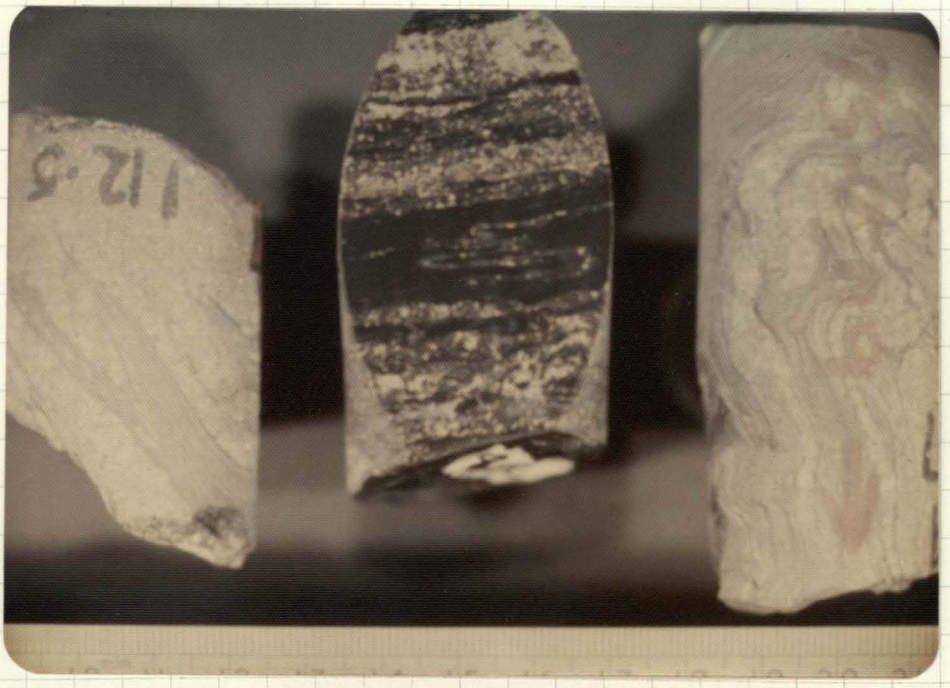

FIGURE 16 FIRST PHASE FOLDS, WITH SECOND PHASE TIGHT REFOLDING OF THE EXAMPLE ON THE RIGHT.

FIGURE 17 FIRST PHASE FOLD (FIG. 16, CENTRE) IN THIN SECTION

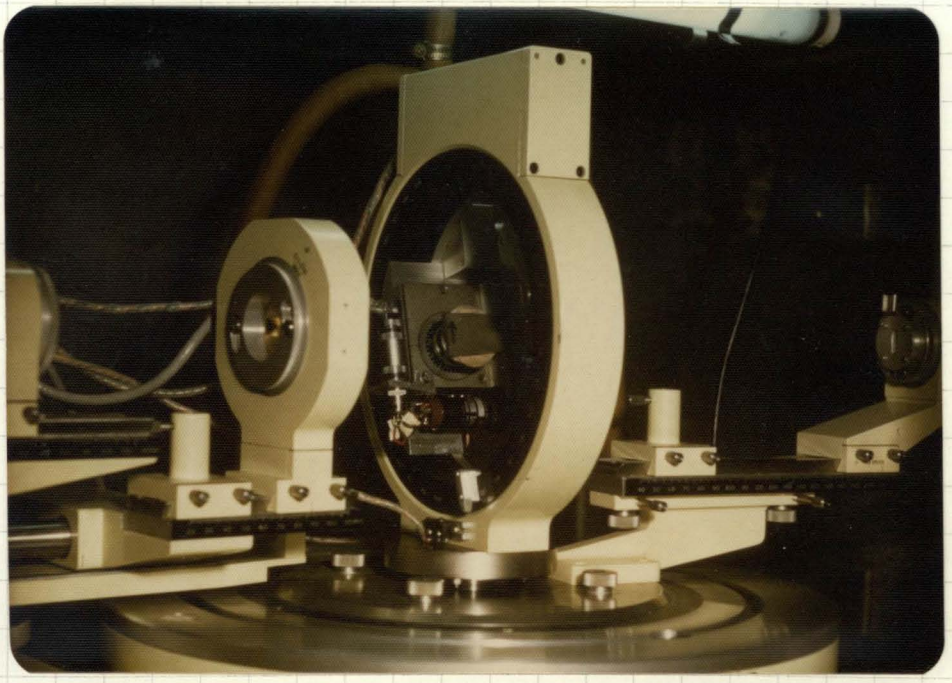

FIGURE 16
THE TEXTURE GONIOMETER ATTACHMENT IN AN X-RAY DIFFRACTOMETER. A pyrrhotite schist specimen, with orientation arrow, is seen mounted on plasticine at the centre of the β rotation circle, with a β tilt of about 20°. Beneath the mount, the α rotation graduations can be seen, and the whole fitting is mounted on the θ rotation circle. The X-ray detector, far right, is mounted on the 2θ rotation circle that surrounds the θ circle, and both circles are aligned with the X-ray source and main slits on the left.

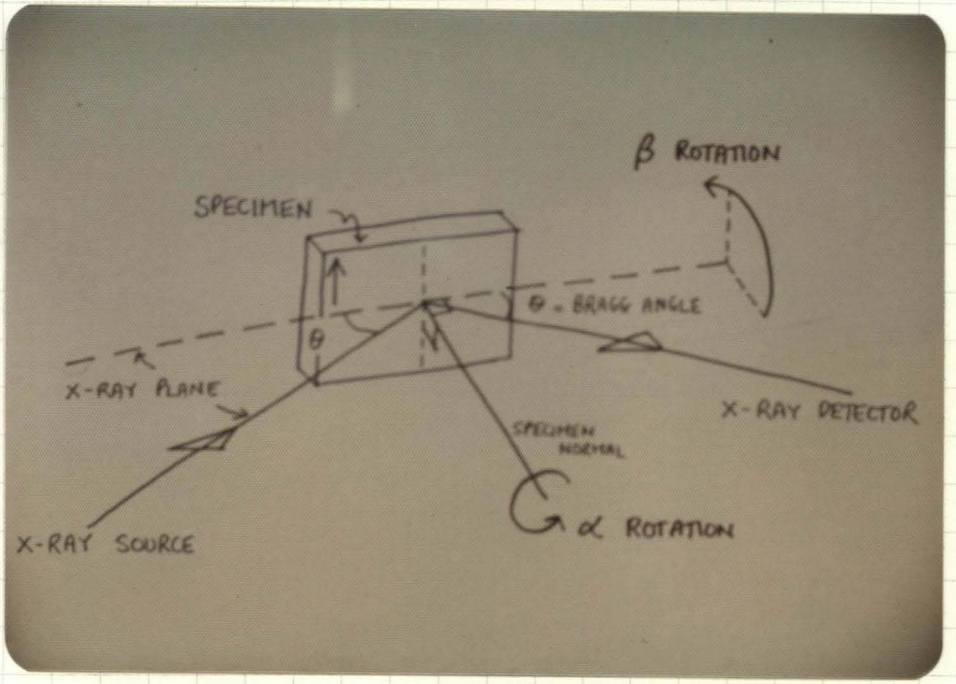

FIGURE 17
TEXTURE GONIOMETER ROTATION SCHEME.

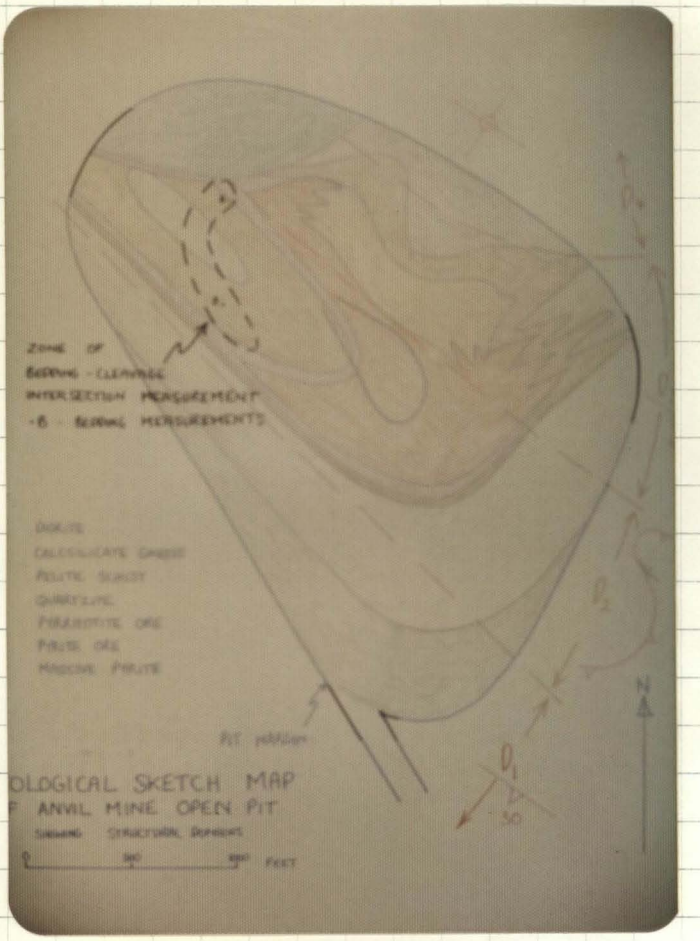
ZONE OF
BEDDING - CLEAVAGE
INTERSECTION MEASUREMENT
+B BEDDING MEASUREMENTS
DIORITE
CALC-SILICATE GNEISS
PELITIC SCHIST
QUARTZITE
PORPHYRITIC ORE
PELITIC ORE
MASSIVE PYRITE
PIT MARGIN
OLOGICAL SKETCH MAP
F ANVIL MINE OPEN PIT
SHOWING STRUCTURAL DOMAINS
FEET
N
D1
A
30

FIGURE 18

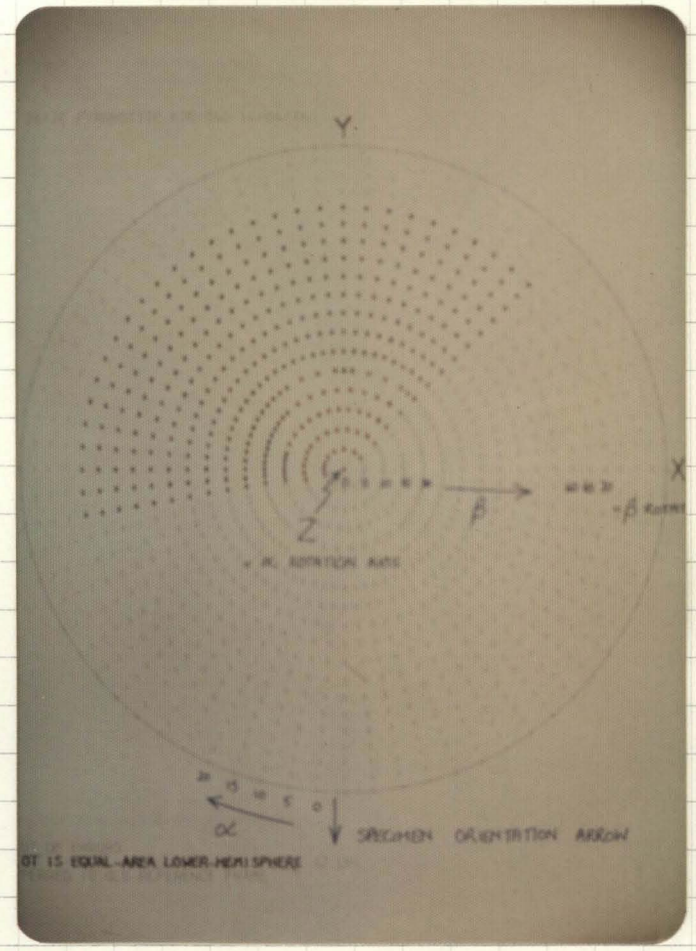

FIGURE 18

POLE FIGURE OUTPUT FROM COMPUTOR CORRECTION AND PLOTTING PROGRAMME. Showing individual (black dots) and averaged (red dots) intensity readings, the α (= Z) and β (= X) rotation axes and graduations, and the specimen orientation arrow.

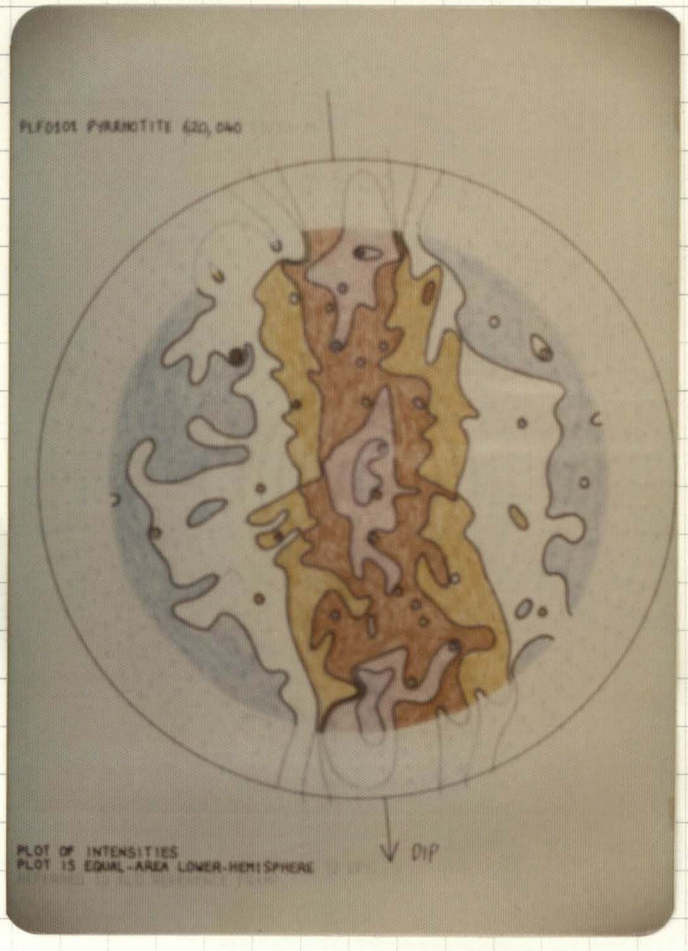

FIGURE 19

POLE FIGURE FOR A FINE-GRAINED PYRRHOTITE SCHIST, SAMPLE PLF0101 Contours are at 0·5, 1·5, 2·5, 3·5, 4·5 and 15·5 times the calculated random fabric intensity for the 620 and 040 faces of monoclinic pyrrhotite. Approximately half a million grains in an area of about four square centimetres were irradiated to produce this pole figure, which is similar to that which might be produced from a very imperfect single crystal.

FIGURE 19

BEDDING STRIPING ON THE EARLY CLEAVAGE IN THE QUARTZITE

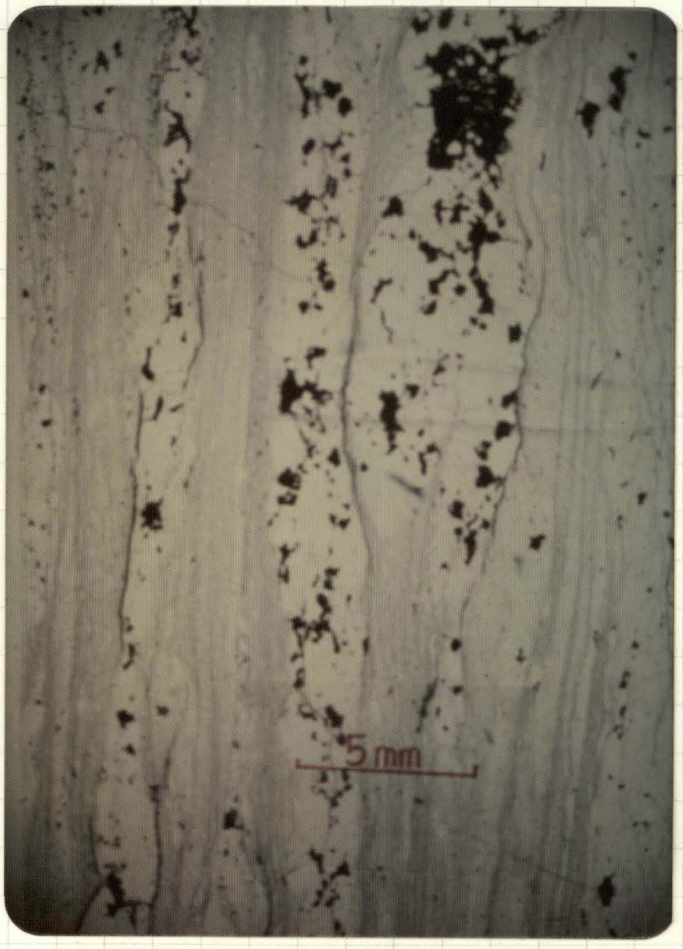

lower case → THIN SECTION OF QUARTZITE SHOWING BEDDING STRIPING. SECTION IS NORMAL TO THE BEDDING - CLEAVAGE INTERSECTION and shows coarse quartz-pyrite beds transposed almost parallel to the penetrative cleavage in the fine grained muscovitic quartzite.

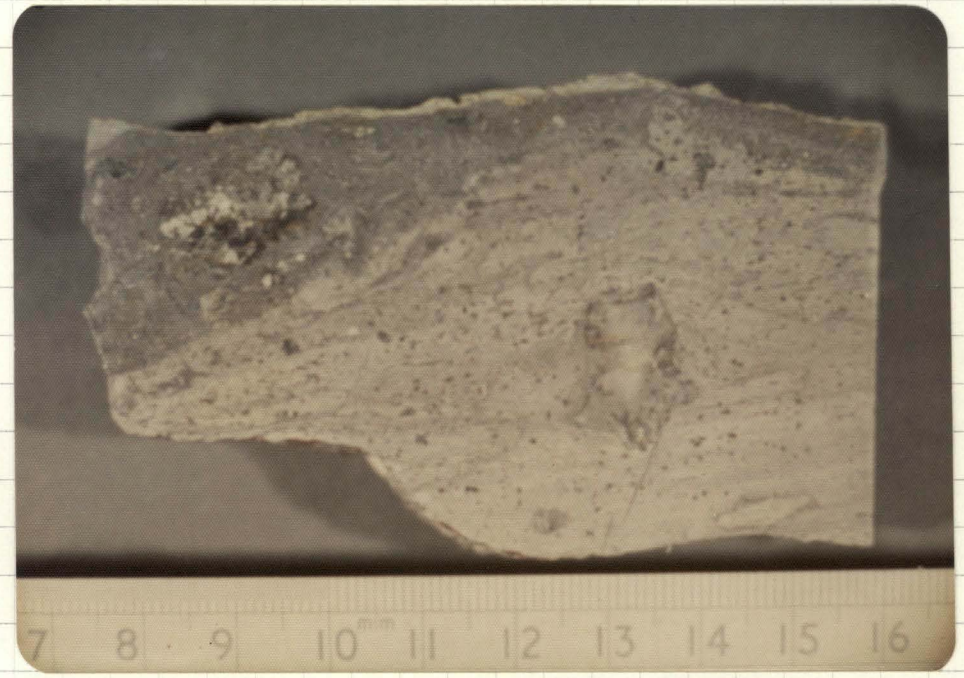

FIGURE 20
PYRRHOTITE SCHIST SAMPLE PLF0101, from which Figure 19 was produced. The upper surface is an early schistosity plane at the

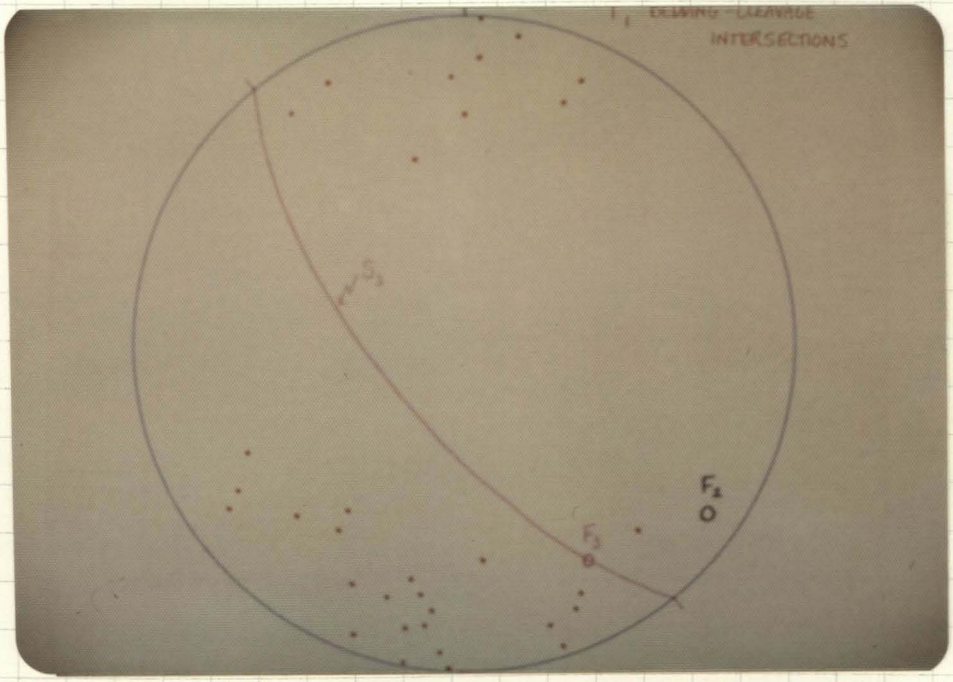

FIG 20 : FIRST PHASE BEDDING - CLEAVAGE INTERSECTIONS.
The mean axial plunges of second and third phase folds and the mean axial plane of third phase folds are also shown.

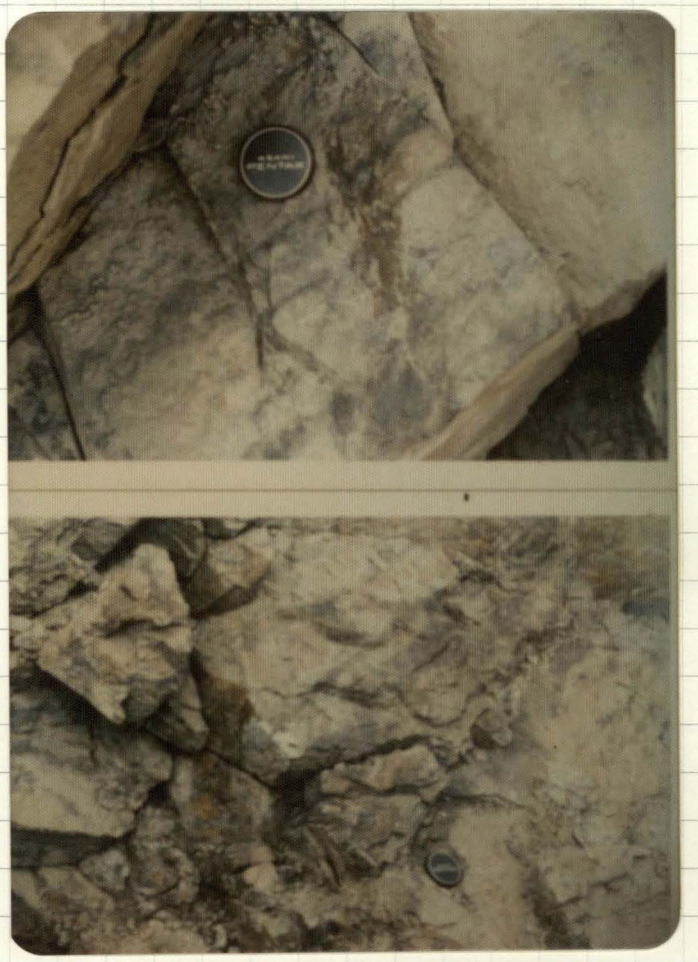

FIGURE 21

BEDDING OBLIQUE TO EARLY CLEAVAGE IN QUARTZITE
The lens caps lie on the cleavage surface

THIN SECTION OF SAMPLE FROM TOP EXPOSURE ABOVE
An asymmetric fold in a coarse quartz-pyrite bed has the early cleavage crudely axial planar.

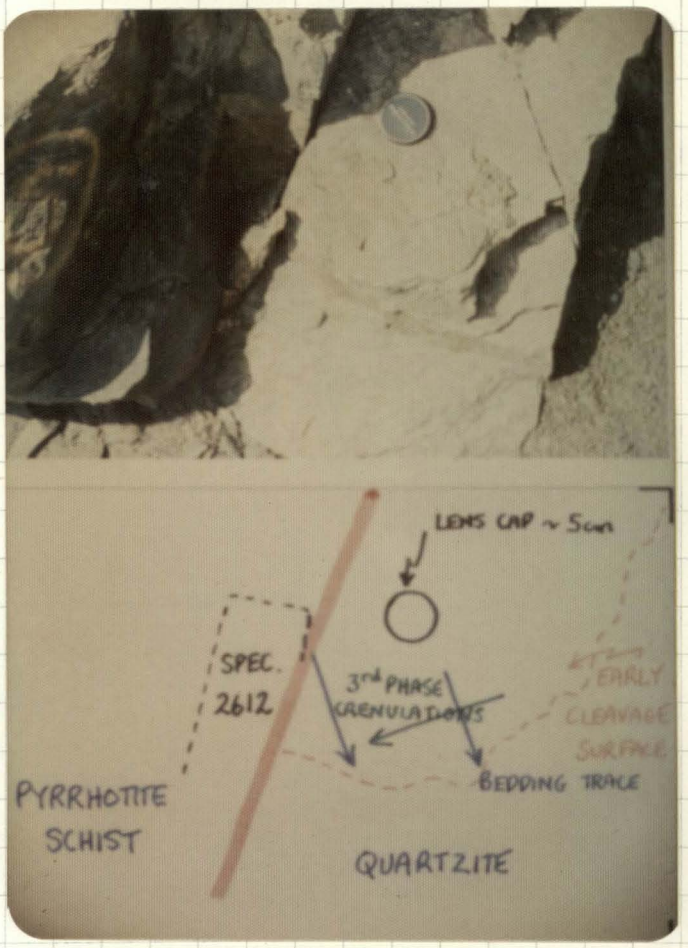

FIGURE 21
LOCALITY ON WEST WALL OF PIT SHOWING PYRRHOTITE SCHIST IN FAULT CONTACT WITH QUARTZITE. Also showing position of sample PL 2612.

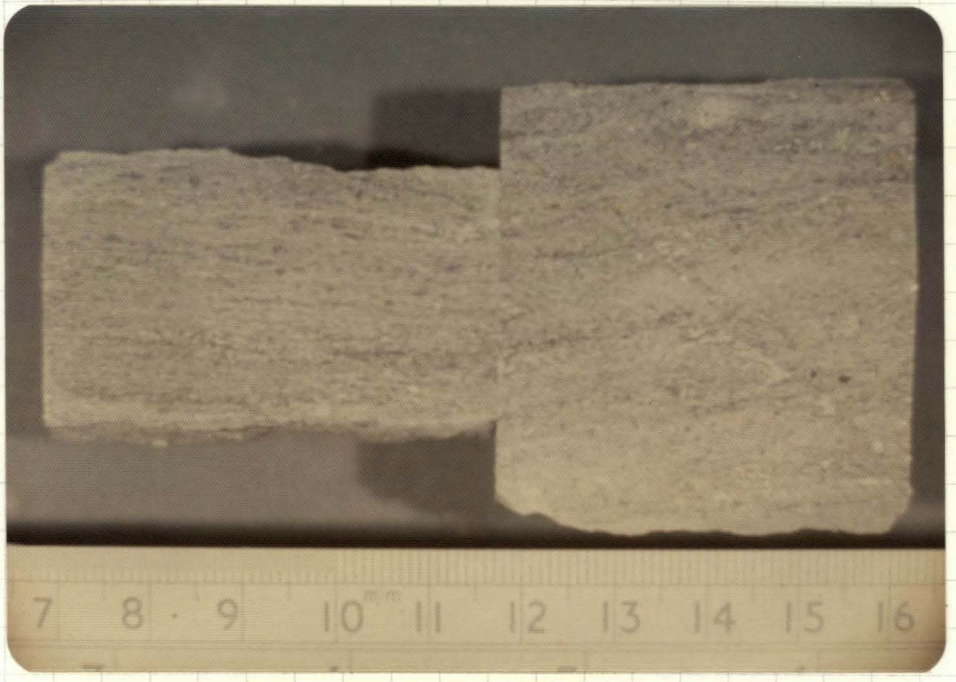

FIGURE 22
PYRRHOTITE SCHIST SAMPLE PL2612, showing a strong planar fabric in a cut parallel to the probable movement direction (parallel to dip direction of schistosity) at left, and a weaker fabric in a cut normal to the movement direction.

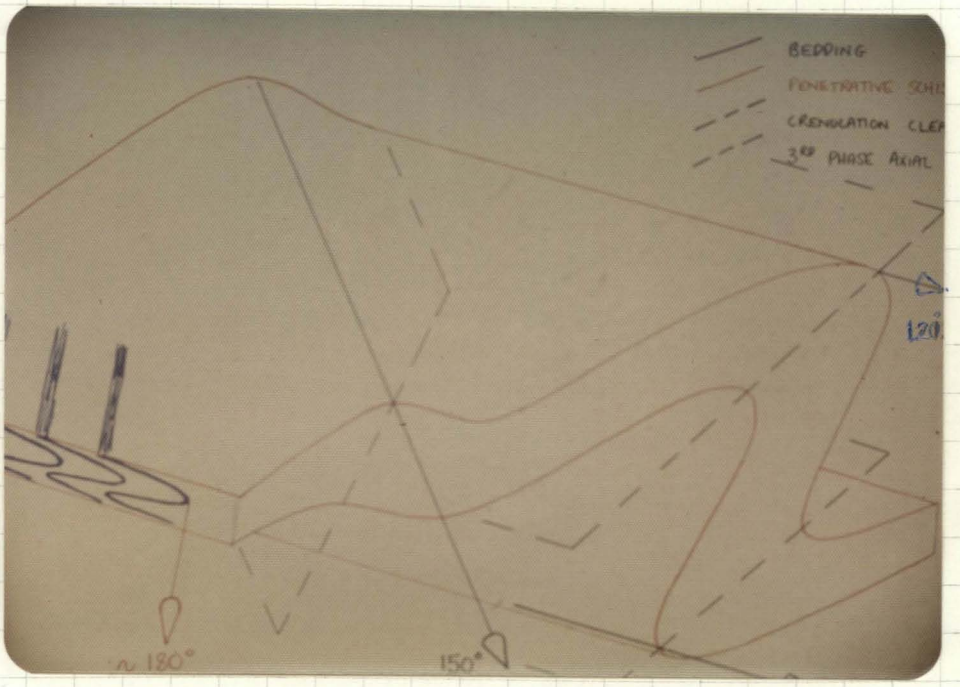

FIGURE 22

SUMMARY SKETCH SHOWING GEOMETRY OF DEPOSIT.

FIGURE 23
PYRRHOTITE SCHIST SAMPLE FROM DIAMOND DRILL HOLE 75-2 AT 638 FEET.
The sample is the central part of a zoned dyke-like intrusion consisting of a magnetitic selvedge bounding a chalcopyrite-pyrrhotite zone with a pyrrhotitic core. The cut shows the maximum discordance between foliations in the host rocks and within the dyke and is not normal to the pyrrhotite schistosity which dips toward the reader as shown below.

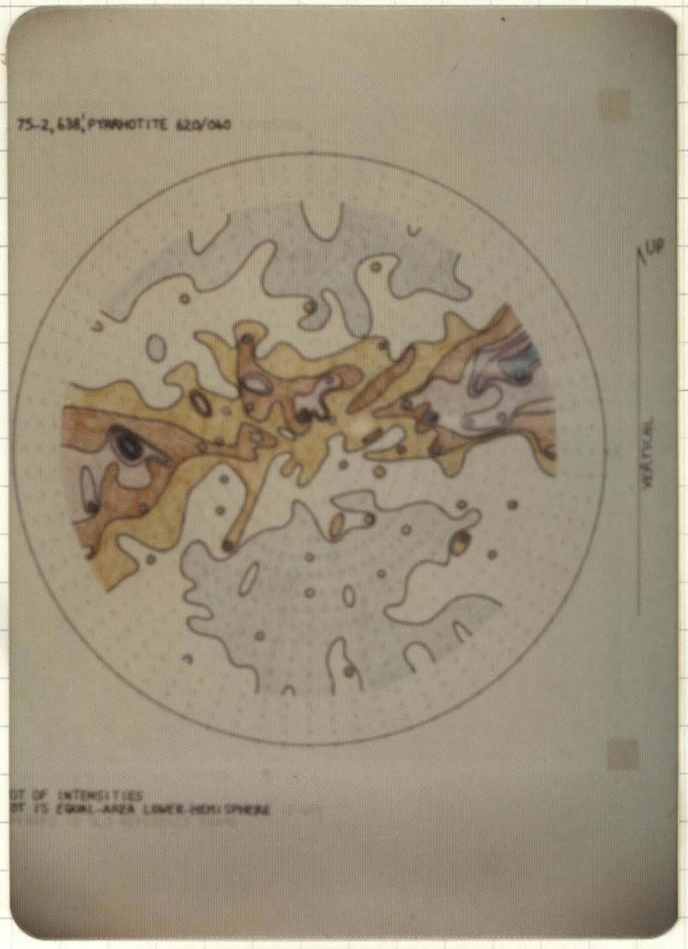

FIGURE 24
POLE FIGURE FOR SAMPLE PLF 75-2, 638'.
Contours as for Figure 19, to a maximum of 7.5 times random fabric intensity for pyrrhotite 620 and 040. Orientation is as for Figure 23 and the components of dip of about 10° to the left and 15° towards the reader are apparent from the attitude of the girdle.

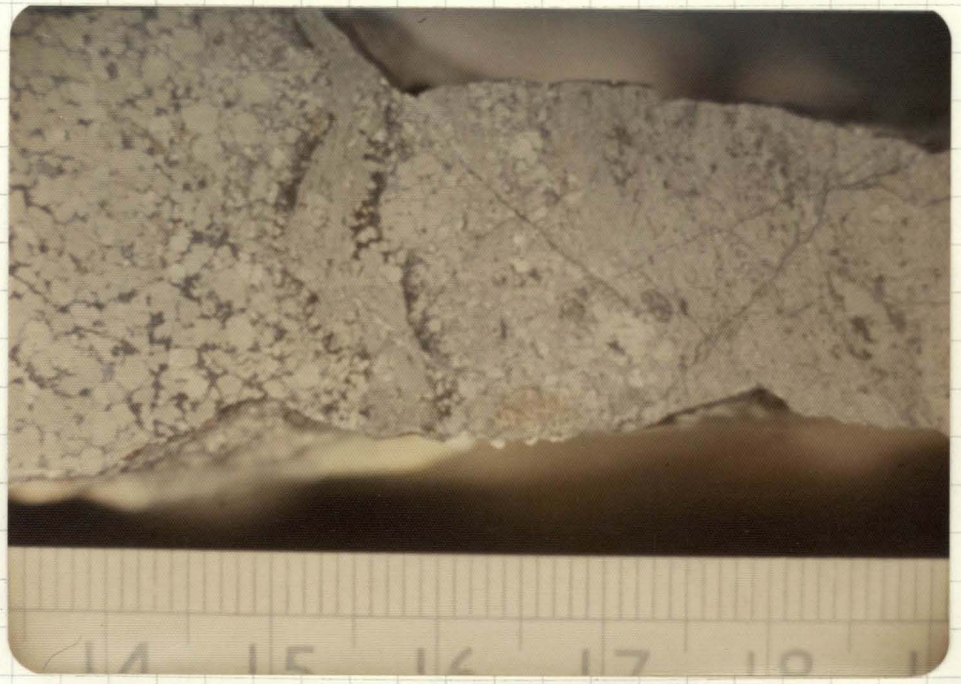

FIGURE 25
CONTACT BETWEEN BANDED GNEISSOSE ORE AND PYRRHOTITE SCHIST, showing :-
a) banded ore
b) cataclased banded ore with pyrite porphyroclasts
c) fine pyrite-marcasite cataclasite
d) pyrrhotite growth within cataclasite
e) pyrrhotite schist

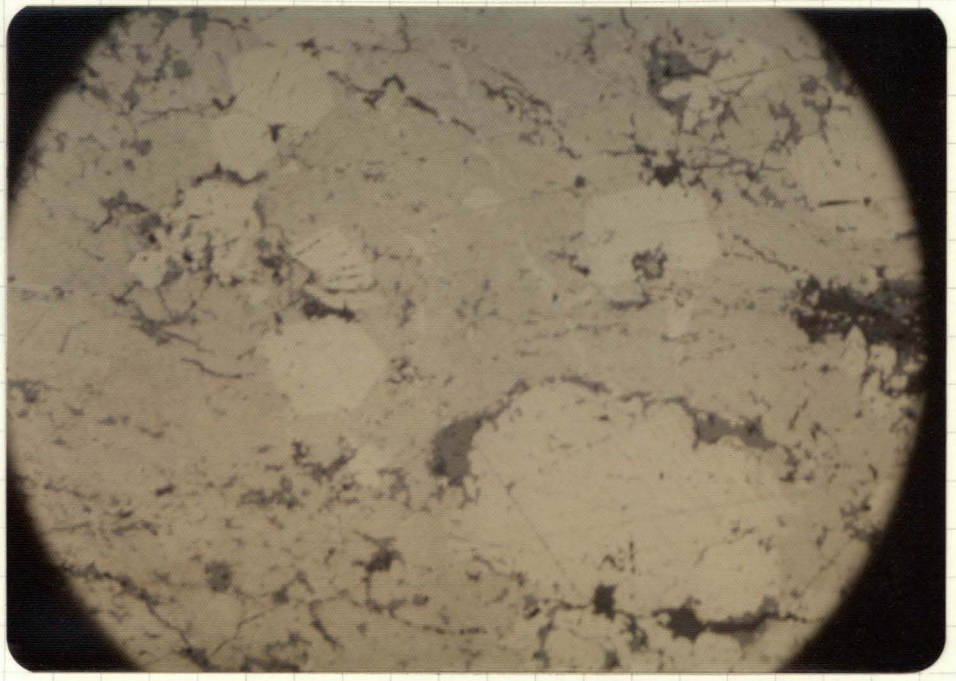

FIGURE 26
FINE PYRITE-MARCASITE CATACLASITE WITH PYRITE PORPHYROCLASTS.

Field of view ~ 1·5 mm.